Chapter-V

5.1 Introduction

$PbTiO_3$ based solid solutions such as (1-x)$Pb(Mg_{1/3}Nb_{2/3})O_3$-x$PbTiO_3$ (PMN-PT) [Lente et al. (2004)], (1-x)$Pb(Ni_{1/3}Nb_{2/3})O_3$-x$PbTiO_3$ (PNN-PT) [Singh et al. (2007)], (1-x)$Pb(Fe_{2/3}W_{1/3})O_3$-x$PbTiO_3$ (PFW-PT) [Mitoseriu et al. (2003)], (1-x)$BiFeO_3$-x$PbTiO_3$ (BF-PT) [Bhattacharjee and Pandey (2010)] etc. are known for strong frequency dispersion in their temperature dependent dielectric response. Some of them exhibit very high dielectric permittivity and strong dielectric relaxation both at cryogenic temperatures as well as high temperatures. Extensive works have been done on the MPB solid solutions for dielectric characterization at higher temperatures in order to understand the nature of phase transition in the vicinity of MPB. However, the dielectric studies at cryogenic temperatures have not got much attention. Only few reports are there on dielectric relaxation in MPB ceramics at cryogenic temperatures. Single crystals of (1-x)$Pb(Zn_{1/3}Nb_{1/3})O_3$-x$PbTiO_3$ [Yu et al. (2003)] and (1-x)$Pb(Mg_{1/2}Nb_{1/3})O_3$-x$PbTiO_3$ [Lente et al. (2004)] have been reported to exhibit the dielectric relaxation at cryogenic temperatures well below the transition temperature (T_c) of ferroelectric to paraelectric state. The origin of dielectric anomaly at cryogenic temperatures is a question of debate also. Two models have been proposed to understand the origin of dielectric anomaly at cryogenic temperatures. The first one [Guo et al. (1990); Lente et al. 2004] is based on the polarization fluctuations by chemical heterogeneities, however other [Viehland (2000); Priya et al. (2002)] reports it to be due to fractural cluster inside the normal ferroelectric domain. Singh et al [Singh et al. (2007)] have reported that

this dielectric anomaly is indirectly linked with the structural phase transition at lower temperatures. However, the model of Singh et al [Singh et al. (2007)] will not explain the dielectric relaxational peak at cryogenic temperatures in the cubic and tetragonal compositions that do not exhibit the low temperature structural transformations.

At high temperatures, frequency dependent dielectric anomaly has got much attention due to its diffuse phase transition (DPT) [Balagurov and Vaks (1994)] and relaxor ferroelectric [Bokov and Ye (2006)] nature with huge dielectric response [Fu et al. (2009)]. As discussed in Chapter I (Section 1.4), relaxors are usually disordered ferroelectric systems [Bokov and Ye (2006)]. The dielectric relaxation which is very fast above peak temperature (T_m), slows down below T_m, signifying the relaxor freezing [Pirc and Blinc (2007)]. In particular, on cooling below the Burns temperature (T_B) [Burns and Dacol (1983)], which is much above the T_m, the relaxor ergodic state transforms in to the non-ergodic state with appearance of randomly oriented polar nano regions (PNRs) due to charge fluctuation. On further cooling below T_m, the size of PNR is increased and frozen which results in huge polarization. The temperature at which this freezing occurs is called Vogel-Fulcher freezing temperature (T_{vf}) [Bokov and Ye (2006)]. The Vogel-Fulcher freezing may or may not be accompanied with the structural phase transition while cooling from high temperature. When the randomly oriented polar nanoregions are frozen at T_{vf}, one may expect that there is no entity to get frozen again to show another T_{vf} at further lower temperatures. However the problem becomes complex when a material exhibits two

relaxational freezing and two T_{vf}, one above room temperature and other at cryogenic temperatures.

In this Chapter, we have investigated temperature dependent phase transition in selected compositions of BNT-PT using temperature dependent dielectric and XRD studies. Different compositions of BNT-PT across MPB were selected with pseudocubic, monoclinic and tetragonal structures at room temperature to understand the difference in their dielectric and phase transition behaviour. Dielectric studies both at high temperatures and cryogenic temperatures for the composition range $0.35 \leq x \leq 0.55$ of BNT-PT solid solution reveal that all the compositions across MPB show strong dielectric relaxational peak and Vogel-Fulcher freezing below room temperature. In contrast, only pseudocubic and MPB compositions show dielectric relaxation and Vogel-Fulcher freezing above room temperature. The tetragonal compositions exhibit normal ferroelectric like phase transition to paraelectric phase. Temperature dependent XRD studies do not show clear splitting corresponding to any low temperature structural transition. However, temperature dependence of unit cell volume below room temperature exhibits an anomaly around Vogel-Fulcher freezing temperature.

5.2. Experimental Details

Samples in the present work were prepared by conventional solid state ceramic method. The experimental details are described in Chapter II. Temperature dependent dielectric measurements on silver electroded pellet samples were carried out using Novocontrol, Alpha-A high performance

frequency analyzer at the heating/cooling rate of 1^0C per min. The low and high temperature dielectric data were collected in different sample cells. The temperature of the sample was controlled by Eurotherm programmable temperature controller with an accuracy of $\pm1^0$C for high temperature measurements. Low-temperature dielectric measurements were carried out using a frequency-response analyzer (Novocontrol TB-Analyzer). For cooling the sample down to 5K, a closed-cycle refrigerator with He-gas exchange attachment was used. Temperature-dependent capacitance data was measured in the frequency range of 5Hz to $7x10^5$Hz, with a heating rate of 0.8K/min in the range from 5K to 300K.

5.3. Results and Discussion:

5.3.1. Low Temperature Dielectric Studies

Fig.5.1 depicts the temperature dependence of real ($\varepsilon^{/}$), imaginary ($\varepsilon^{//}$) parts of permittivity and loss tangent (tanδ) in the temperature range 5K to 300K measured at different frequencies from 5Hz to $7x10^5$Hz for the compositions with x=0.35, 0.40, 0.45, 0.49, 0.52 and 0.55. As shown in this Figure, for all the compositions, $\varepsilon^{/}$ does not exhibit any visible anomaly on cooling from room temperature to 5K, but strong frequency dispersion in large temperature interval is clearly seen. Anomaly in the imaginary part of dielectric permittivity is observed on lowering the temperature from room temperature to 5K with significant frequency dispersion. The peak temperature ($T^{//}_{m1}$) of the $\varepsilon^{//}$ maxima shifts towards the higher temperature side with increasing the frequency from 5Hz to $7x10^5$Hz. The anomaly in the tanδ is more clearly visible and on lowering

the temperature the peak maxima shifts towards the higher temperature side on increasing the frequency. All these features suggest the relaxor behaviour in these compositions below room temperature. For a given frequency, the $T^{//}_{m1}$ (at low temperatures) of the $\varepsilon^{//}$ and tanδ are shifting towards the lower temperature side on increasing the concentration of $PbTiO_3$ in the composition range x=0.35-0.55.

The temperature dependence of relaxation time (τ) has been modeled using Arrhenius [Bokov and Ye (2006); Singh et al. (2008)] and Vogel-Fulcher relations [Vogel (1921); Fulcher (1925)] according to equations (5.1) and (5.2), respectively.

$$\ln(\tau) = \ln(\tau_o) + \frac{Ea}{kT} \quad \ldots\ldots\ldots\ldots\ldots\ldots \quad (5.1)$$

$$\ln(\tau) = \ln(\tau_o) + \frac{Ea}{k(T-Tvf)} \quad \ldots\ldots\ldots\ldots \quad (5.2)$$

where, E_a correspond to the activation energy, T_{vf} is the Vogal-Fulcher freezing temperature and k is the Boltzmann constant.

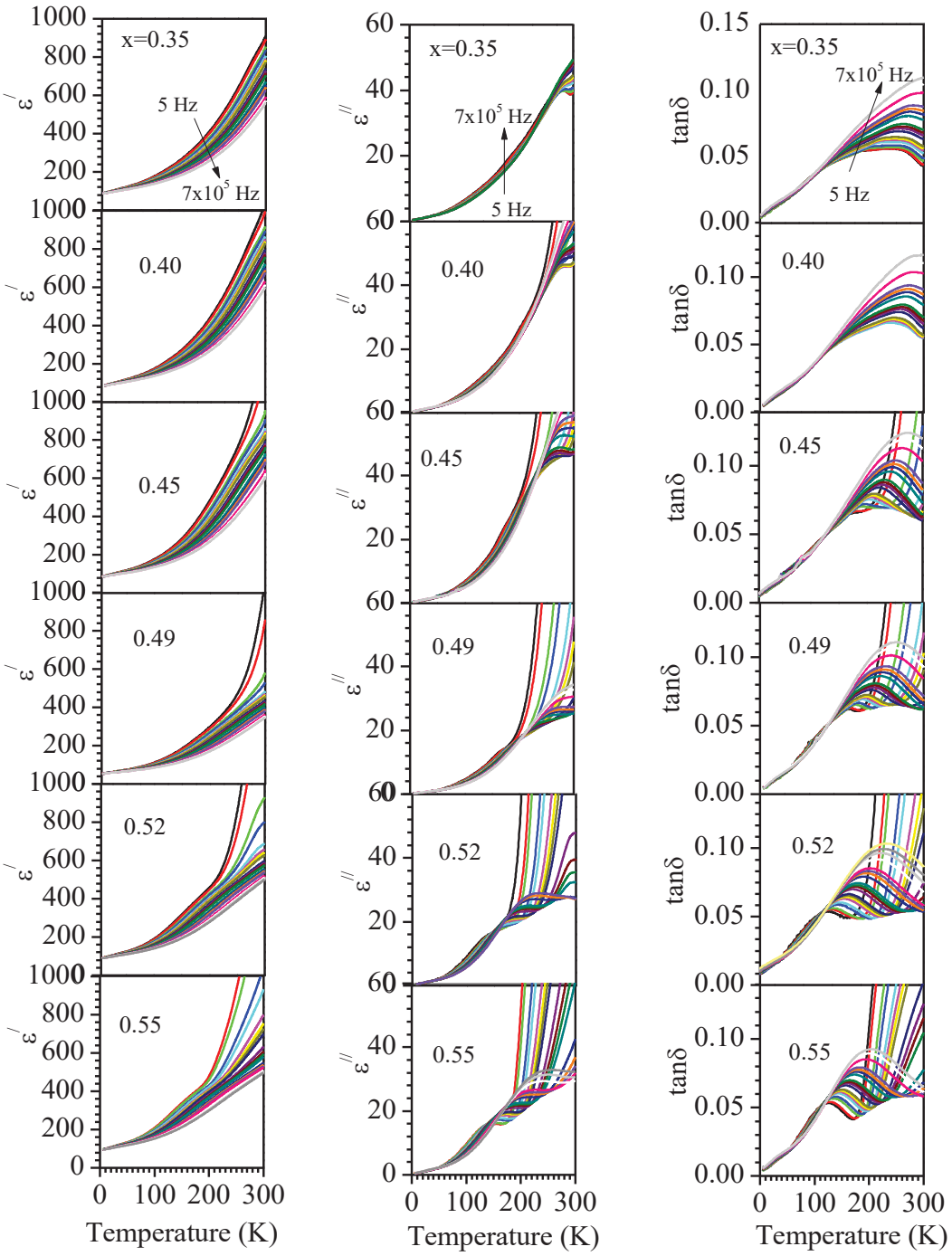

Fig.5.1. Temperature dependence of real ($\varepsilon^{/}$), imaginary ($\varepsilon^{//}$) parts of permittivity and loss tangent (tanδ) in the temperature range 5K to 300K measured at different frequencies from 5Hz to $7x10^5$Hz for the compositions with x=0.35, 0.40, 0.45, 0.49, 0.52 and 0.55.

The Arrhenius and Vogel-Fulcher fits for the relaxation time, as obtained from the $\varepsilon^{//}(T)$ data is shown in Figs.5.2 (a,b,c) for the compositions with x=0.35, 0.49 and 0.55. Non-linear curve shown in the inset of Figs.5.2 (a,b,c) rules out the Arrhenius type behaviour. Satisfactory fit is obtained for Vogel-Fulcher relation. For the composition with x=0.55, the Vogel-Fulcher relation results the activation energy E_a ~0.1336eV, relaxation time $\tau \sim 7.5x10^{-10}$ s and Vogel-Fulcher freezing temperature of 75K. However, E_a ~$1.54x10^{-3}$eV, $\tau \sim 0.26x10^{-5}$s and T_{Vf} ~223K are obtained for the composition with x=0.35. The lower value of activation energy for the composition with x=0.35 than that of x=0.55 reveals that dipolar excitation requires less energy because it is occurring at the higher temperature in 0.65BNT-0.35PT. The composition dependent variation of T_{Vf} is shown in Fig.5.3. The T_{vf} shifts towards lower temperature side with increasing the $PbTiO_3$ concentration in (1-x)BNT-xPT. As shown in Fig.5.1 (for $\varepsilon^{//}$and tanδ), dielectric relaxation starts just below the room temperature for the composition with x=0.35 while it occurs around ~150K for the composition with x=0.55. Obviously, similar trend should be followed by T_{Vf} also. Substitution of normal ferroelectric $PbTiO_3$ is expected to weaken the relaxor behaviour that's why the dielectric anomaly is shifting to lower temperature side with increasing the $PbTiO_3$ concentration.

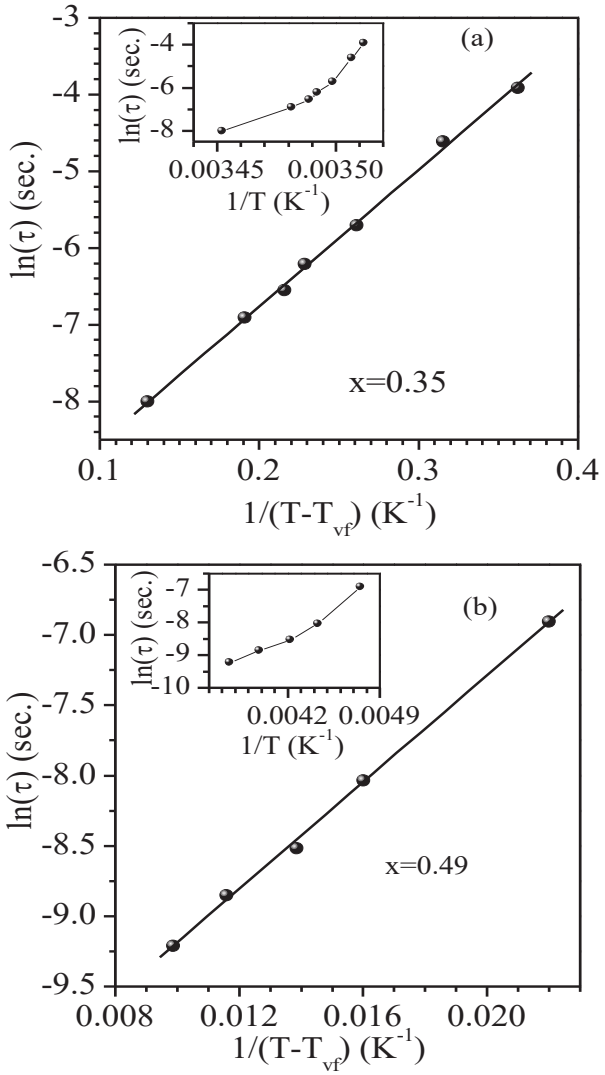

Fig.5.2. Arrhenius (shown in inset) and Vogel-Fulcher fits for the relaxation time, as obtained from the $\varepsilon^{//}(T)$ data for the compositions with (a) x=0.35 and (b) 0.49. Linear fit is obtained for the Vogel-Fulcher freezing.

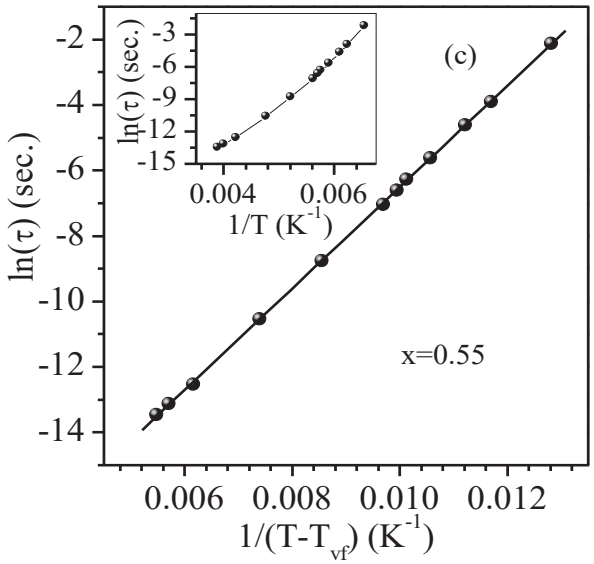

Fig.5.2.(c) Arrhenius (shown in inset) and Vogel-Fulcher fits for the relaxation time, as obtained from the $\varepsilon^{//}(T)$ data for the compositions with x=0.55. Linear fit is obtained for the Vogel-Fulcher freezing.

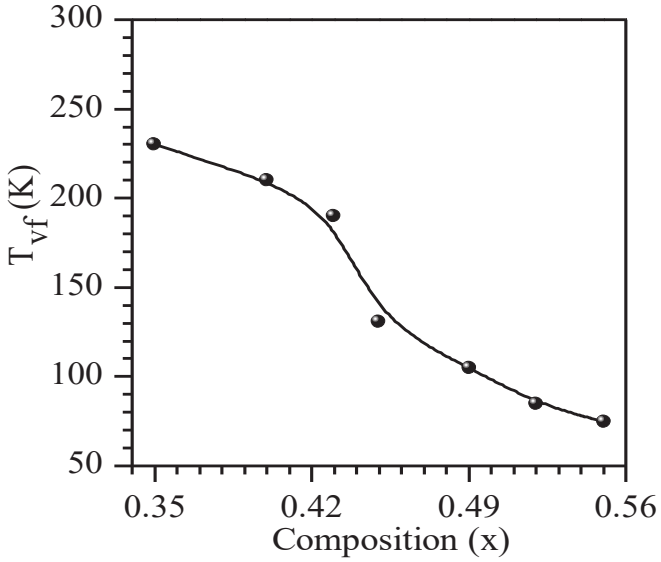

Fig.5.3. Variations of Vogel-Fulcher freezing temperature T_{Vf} with composition for x=0.35, 0.40, 0.45, 0.49, 0.52 and 0.55 below room temperature.

5.3.2. Low Temperature XRD Studies

Some of the authors have reported that the anomaly in the dielectric relaxation below room temperature is associated with polarization fluctuations caused by chemical heterogeneities [Guo et al. (1990); Lente et al. 2004] or due to fractural clusters inside the normal ferroelectric domains [Viehland (2000); Priya et al. (2002)]. They have argued that this dielectric relaxation is not associated with any structural phase transition. However, Singh et al [Singh et al. (2007)] have reported that dielectric relaxation at cryogenic temperatures is associated with lower symmetry structural phase transition. To investigate the possible reason of dielectric relaxation at cryogenic temperatures in (1-x)BNT-xPT, we carried out low temperature XRD studies on (1-x)BNT-xPT compositions with x=0.40, 0.43 and 0.49 in the temperature range 23K-300K. We did not observe any clear signature of structural phase transition in diffraction pattern recorded at lower temperatures. XRD profiles for pseudocubic (110) and (111) reflections are shown in Figs.5.4 (a-c) for the compositions with x=0.40, 0.43 and 0.49. Only the shift in the peak positions is observed for all the reflections. We have plotted in Figs5.5(a-c) the variation of the unit cell volume with temperature in the temperature range 23K to 300K for the composition with x=0.40, 0.43 and 0.49 as shown. Clear anomaly in the unit cell volume is observed around T_{vf}. More investigations will be needed in future to understand the link between anomaly in the unit cell volume and Vogel-Fulcher freezing temperature.

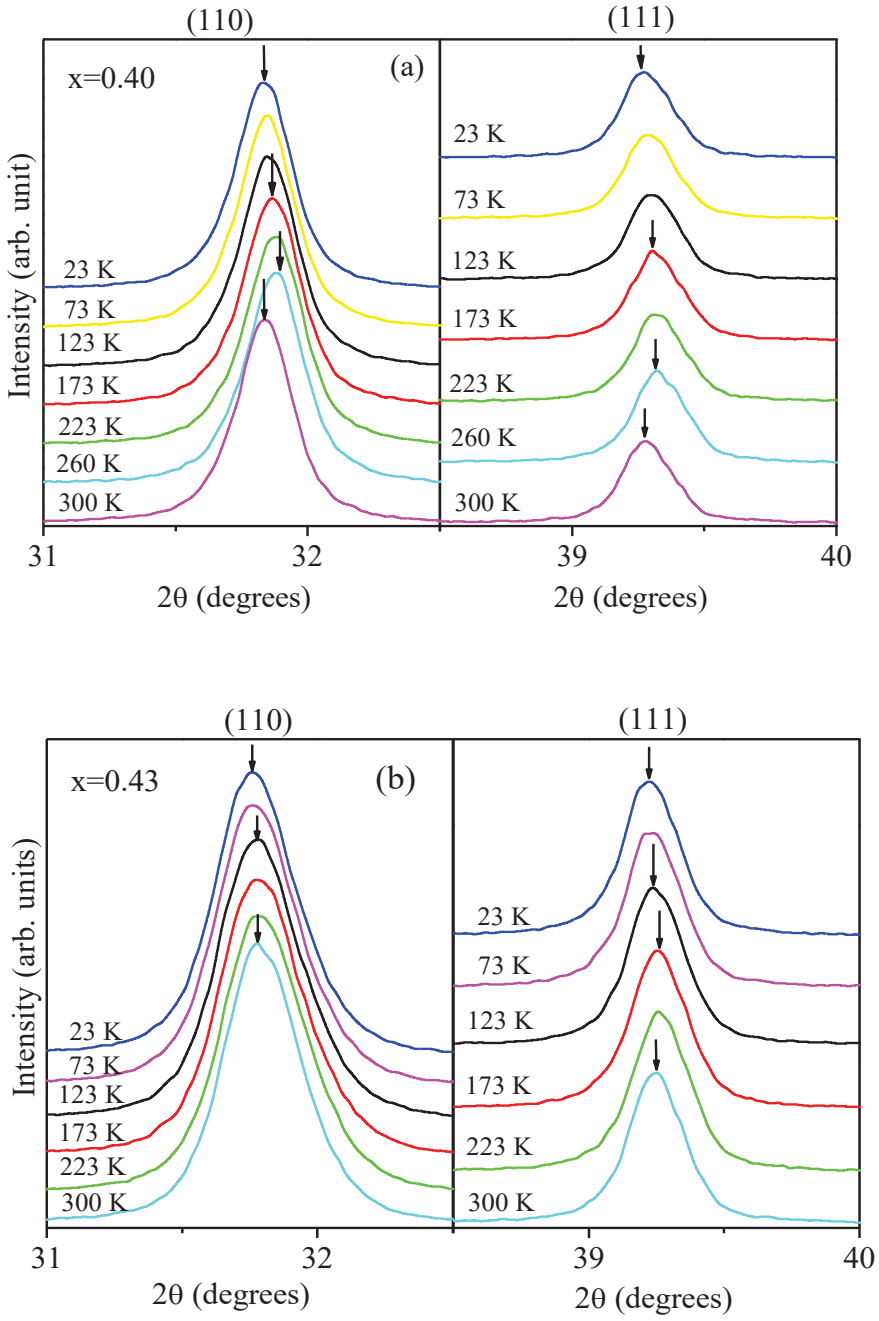

Fig.5.4. Temperature evolution of the pseudocubic (110) and (111) XRD profiles for the compositions with (a) x= 0.40 and (b) x=0.43.

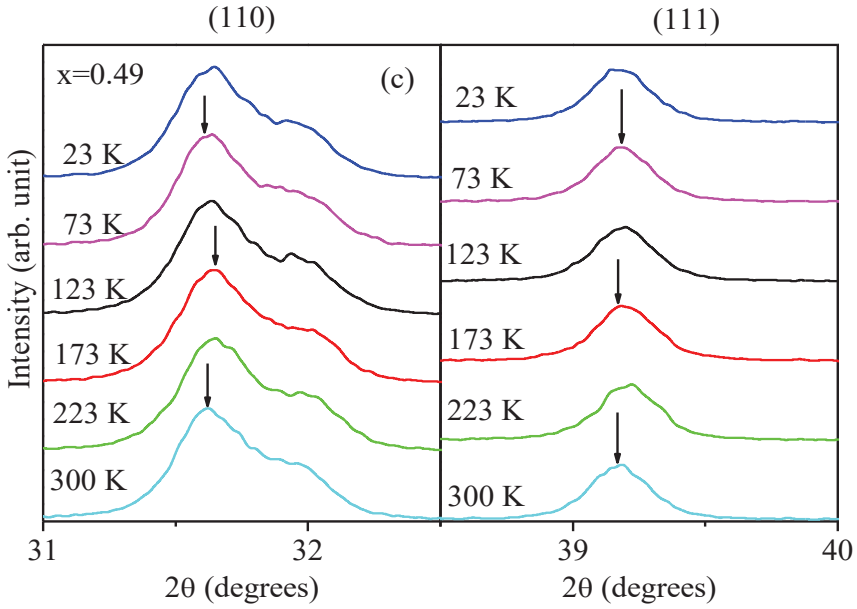

Fig.5.4. (c) Temperature evolution of the pseudocubic (110) and (111) XRD profiles for the compositions with x= 0.49 in the temperature range 23K-300K.

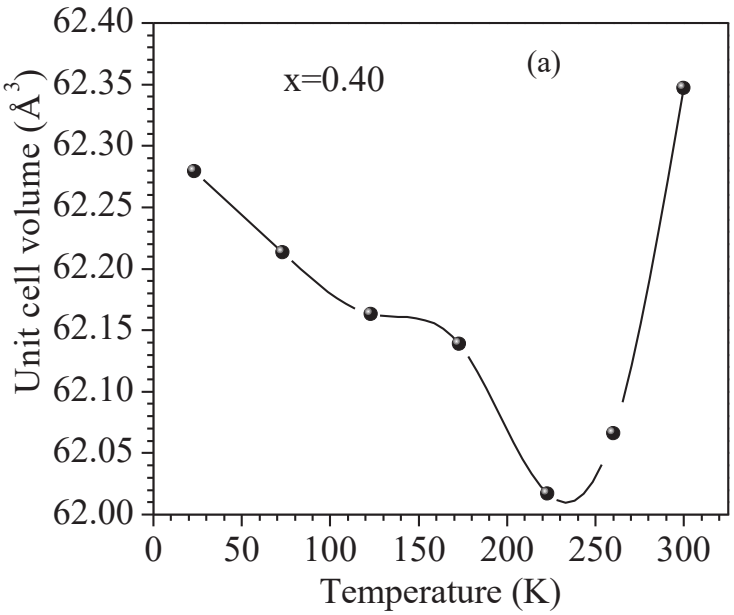

Fig.5.5.(a) Variations of the unit cell volume in the temperature range 23K-300K for the compositions with x=0.40.

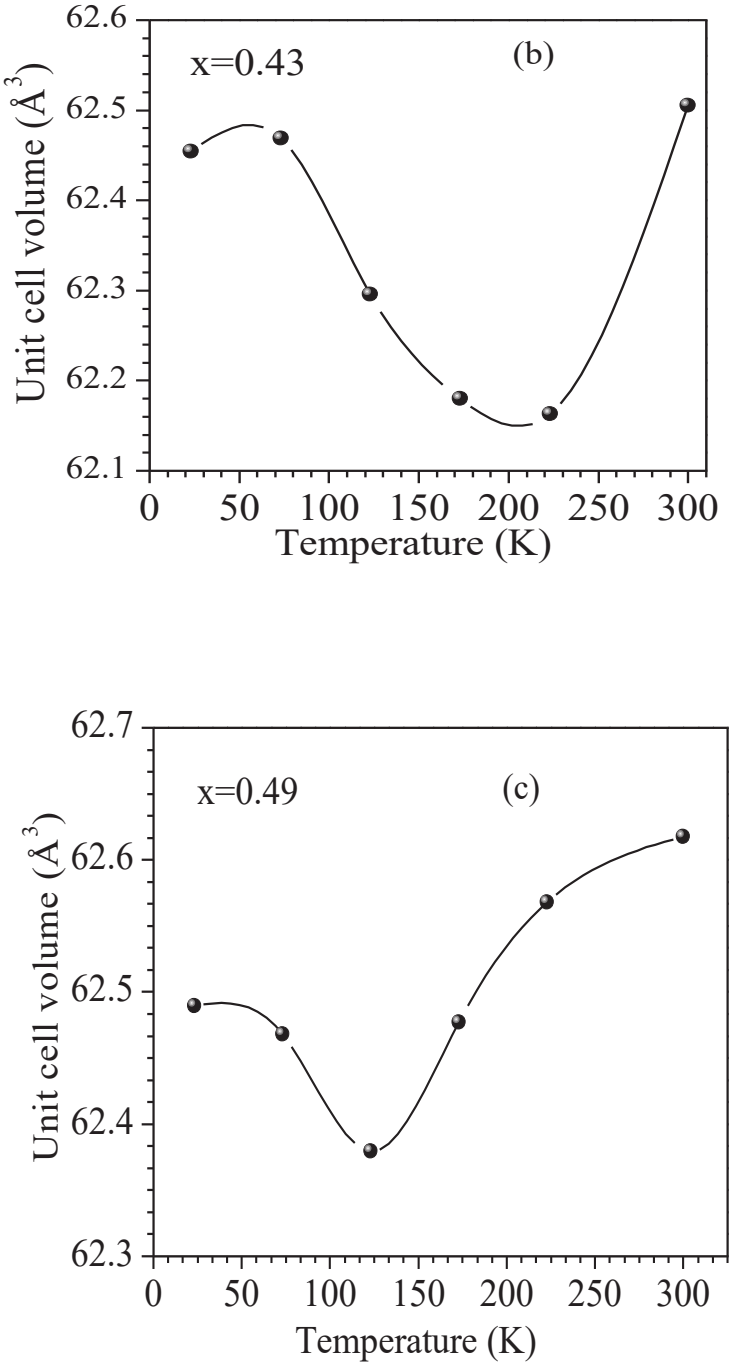

Fig.5.5. Variation of unit cell volume in the temperature range 23K-300K for the compositions with (b) x=0.43 and (c) x=0.49.

5.3.3. High Temperature Dielectric Studies

Temperature dependent dielectric measurements above room temperature on various compositions of BNT-PT across MPB have been done to characterize their phase transition behaviour above room temperature. The compositions with tetragonal and monoclinic structure at room temperature are expected to transform into paraelectric cubic phase at higher temperatures. The compositions with cubic structure at room temperature will not undergo any structural transition. Figs.5.6(a-b) show the temperature variation of the permittivity for the cubic compositions (x=0.35 and 0.38) in the temperature range 300K-750K. Exceptionally high value of permittivity with strong frequency dispersion is seen in these figures. The value of permittivity is ~35000 at 100Hz which continuously gets diffused with increasing the frequency. The temperature variation of the permittivity exhibits large frequency dispersion and the peak temperatures in the real ($T_{m1}^{/}$) and imaginary ($T_{m2}^{//}$) parts of the permittivity do not coincide ($T_{m2}^{//}<T_{m1}^{/}$) suggesting the relaxor nature of transition. Further, the permittivity peaks shift towards the higher temperature side on increasing the measuring frequency for both the real and imaginary parts. For measuring frequency of 100Hz and 300kHz, the value of $T_m^{/}$ is 530K and 605K, respectively signifying strong relaxor nature for the composition with x=0.35. Since this composition is cubic at room temperature the dielectric anomaly above room temperature is not due to any structural change.

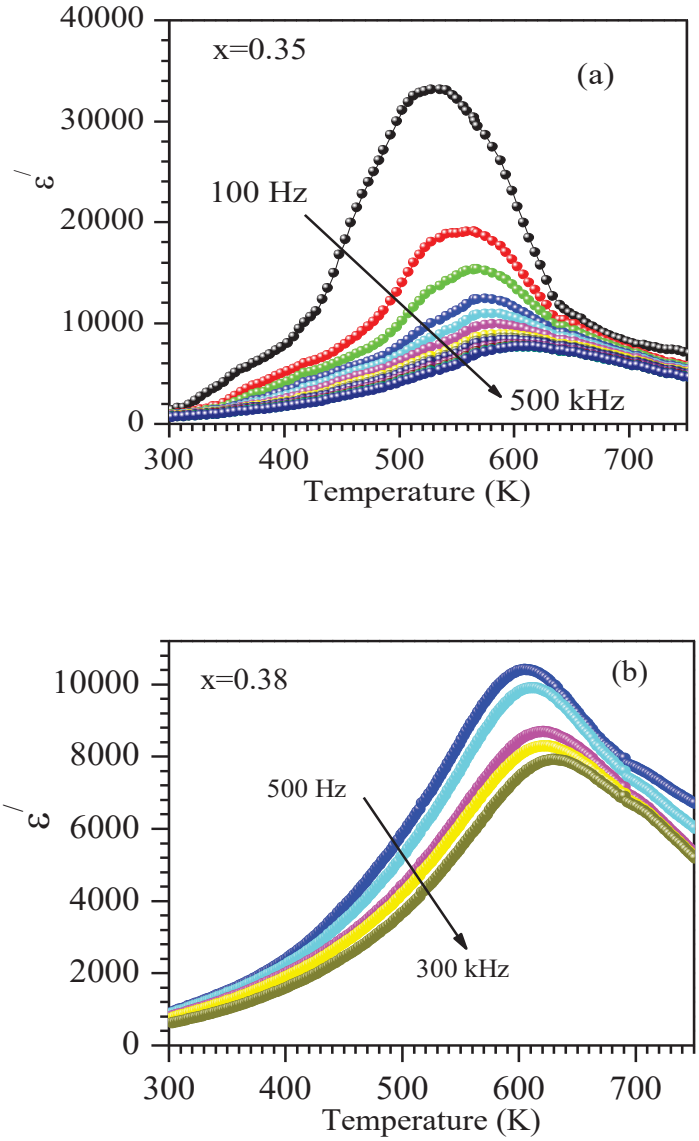

Fig.5.6. Variation of dielectric permittivity (ε') with temperature for the BNT-PT compositions (a) x=0.35, in the frequencies range 100Hz-500kHz and (b) x=0.38, in the frequencies range 500Hz-300kHz.

It is well known that, apart from the relaxational origin, the high value of dielectric permittivity may have contribution from interfacial polarization also [Singh et al. (2003)]. In polycrystalline ceramic samples, interfacial polarization originates from the semiconducting grains and insulating grain boundaries. Polycrystalline oxide ceramic samples are usually sintered at high temperatures. The semiconducting phenomenon in grain boundaries is introduced by the loss of oxygen during sintering of the samples at high temperature, which can be explained using Kroger-Vink notation according to equation (5.3)

$$O_O \longleftrightarrow {}^{1}/_{2}O_2 + V_O^{oo} + 2e^{/} \qquad (5.3)$$

$$2Ni^{3+} + 2e^{/} \longleftrightarrow 2Ni^{2+} \qquad (5.4)$$

Since, the transition metal Ni shows the variable oxidation states (Ni^{2+}, Ni^{3+}) in BNT-PT solid solution [Wu et al. (2002); Zhang et al. (2005); Kang et al. (2013)], the electrons released during sintering are captured by Ni ions. The electron hopping due to change in the ionization state of Ni ions increases the conductivity of grains. During cooling after the sintering, reduction process is started, which only affects the grain boundaries due to the fast process of cooling. The grain boundaries become insulating, however, grains remain semiconducting after sintering. The bound charges at the interface of the grains and grain boundaries generate large space charge polarization and hence large dielectric constant at the lower frequencies [Singh et al. (2003)]. It has been reported that at lower temperatures, the permittivity has major contribution from grains. At the higher temperatures or room temperature grain boundaries are responsible for

giant permittivity response. High value of activation energies in such samples are attributed to more insulating character of grain boundaries than grains which result into high dielectric constant [Thongbai et al. (2008)]. It is obvious that the activation energy is lower for the intrinsic bulk ceramics. It increases if the contribution from the grain boundary increases. It is reported that, in the Ti and Li doped NiO core shell structure, activation energy increases with increasing the concentration of Ti [Thongbai et al. (2008)].

Similar to the compositions with cubic structure at room temperature, significant relaxor nature is seen for the compositions with 0.44 and 0.49 also (Figs.5.6(c-d)). The frequency dispersion gradually diminishes on increasing the $PbTiO_3$ concentration. For the composition with x=0.49, small frequency dispersion is observed and system transforms towards the normal ferroelectric. As shown in Fig.5.6e, the dielectric response for the composition with x=0.55 exhibits complete normal ferroelectric behaviour. To estimate the relative relaxor behaviour of various compositions, we show in Fig.5.7 the peak temperatures at two frequencies and their difference as a function of composition. We denote the dielectric peak temperature as Tm_1 for 1kHz and Tm_2 for 300kHz frequency. It is clear from Fig.5.7 that the difference (Tm_1-Tm_2) between dielectric peak temperatures decreases with increasing PT concentration showing the diminishing relaxor character. The anomaly in the imaginary part of permittivity or loss tangent could not be seen clearly in any of the compositions investigated above. This is because of the enhanced dielectric loss at high temperatures which

overshadow the actual peak. This is shown in Figs.5.8 (a, b) for the composition with x=0.49.

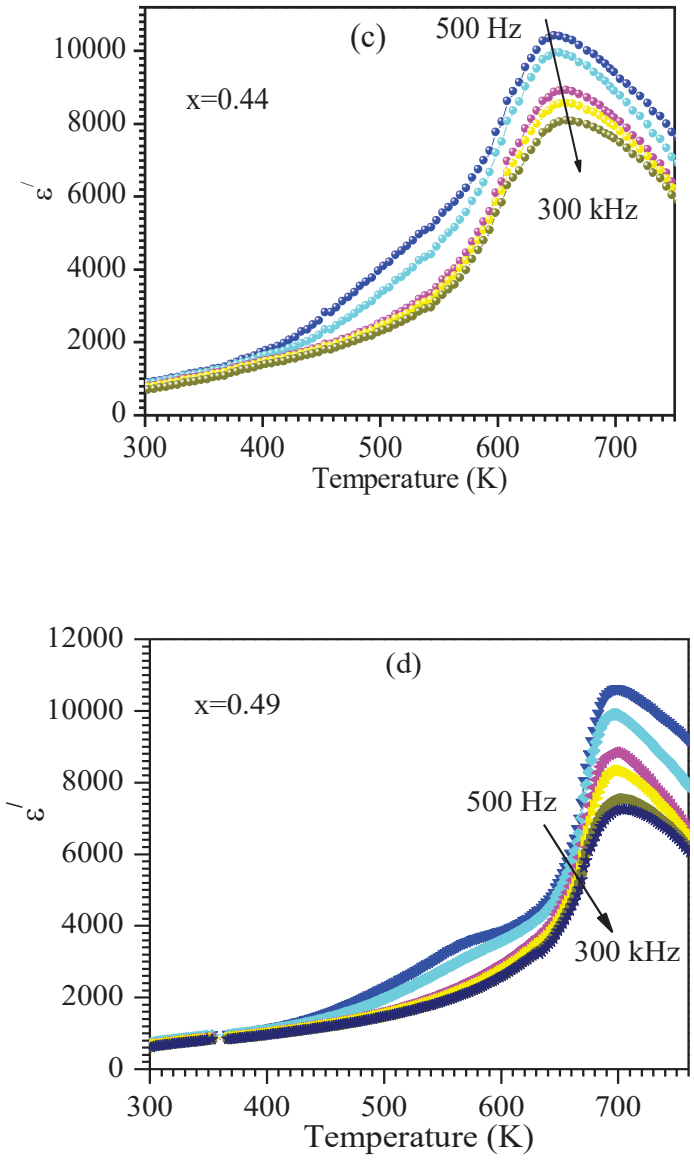

Fig.5.6. Variation of dielectric permittivity (ε') with temperature in the frequencies range 500Hz-300kHz for the BNT-PT compositions (c) x=0.44 and (d) x=0.49.

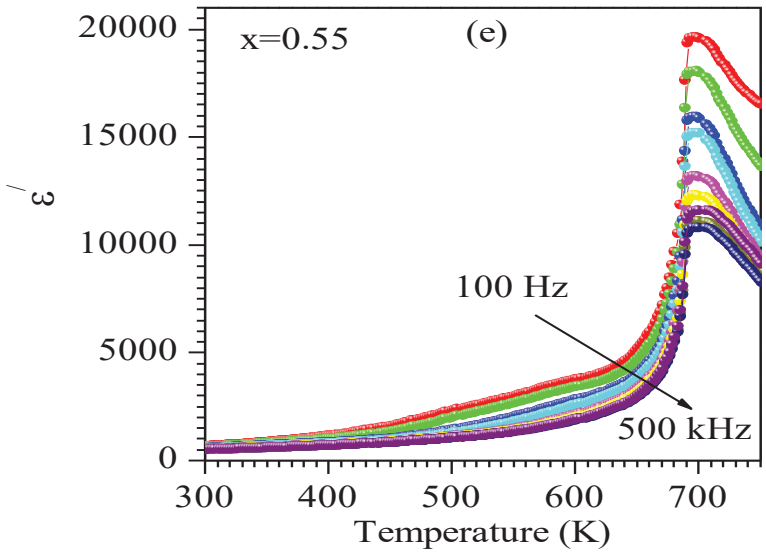

Fig.5.6. (e) Variation of dielectric permittivity ($\varepsilon^{/}$) with temperature in the frequency range 100Hz-500kHz for the BNT-PT composition with x=0.55.

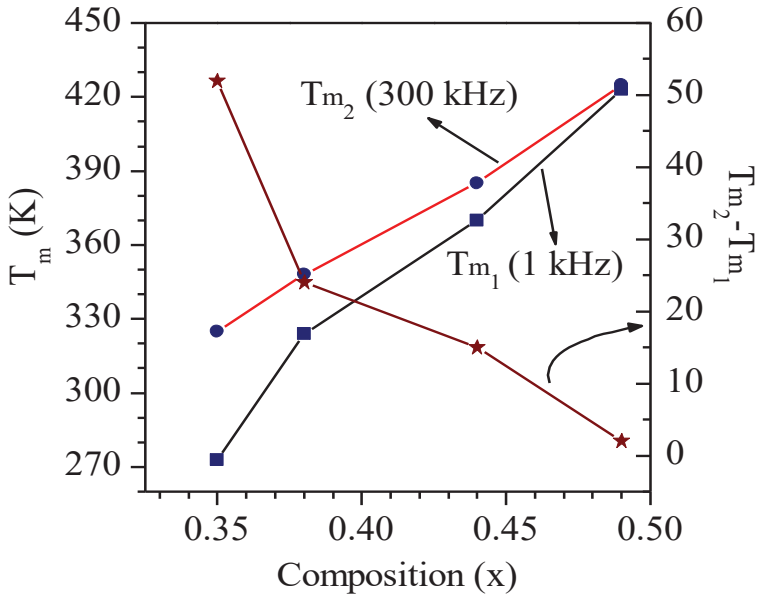

Fig.5.7. Variations of dielectric peak temperatures T_{m1} and T_{m2} at the frequencies 1kHz and 300kHz, respectively. Difference (T_{m1}-T_{m2}) between peak temperatures decreases with increasing PT concentration showing the diminishing relaxor character.

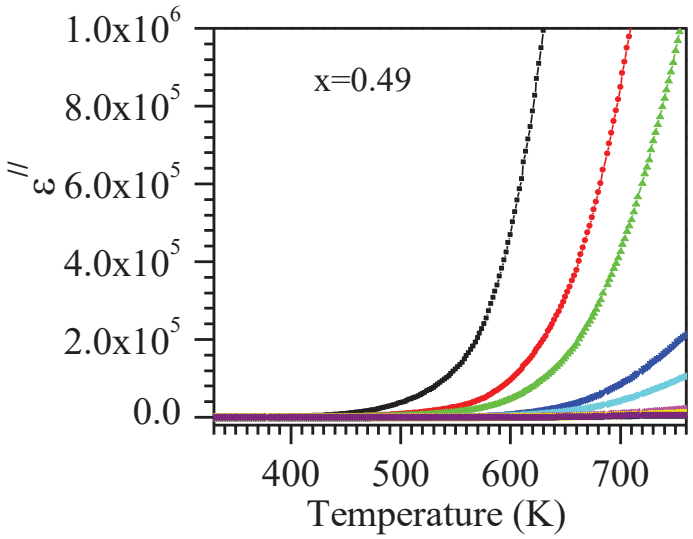

Fig.5.8. (a) Imaginary part of dielectric permittivity for the composition with x=0.49 in the temperature range 300K-750K.

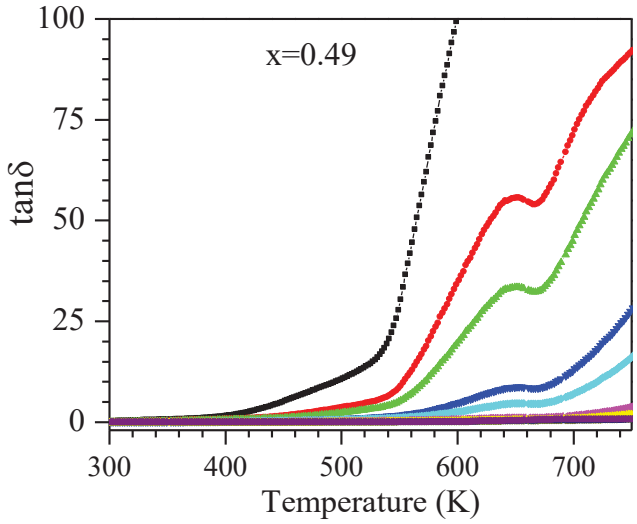

Fig.5.8. (b) Loss tangent for the compositions with x=0.49 in the temperature range 300K-750K.

Figs.5.9(a-d) show the temperature dependence of relaxation time (τ) modelled by using Arrhenius [Bokov and Ye (2006); Singh et al. (2008)] and Vogel-Fulcher relations [Vogel (1921); Fulcher (1925)] given in equations (5.1) and (5.2). The peak temperatures in the real part of the permittivity were used for this fitting. Non-linear curve fit shown in the inset of Figs.5.9(a,b,c,d) rules out the Arrhenius type behaviour. Satisfactory fit is obtained for Vogel-Fulcher relation. The freezing temperature (T_{vf}) increases towards the higher temperature side due to enhancement in T_c on increasing the $PbTiO_3$ concentration. This result is opposite to the results obtained at cryogenic temperatures where T_{vf} shifts towards the lower temperature side. The freezing temperatures for the compositions with x=0.35, 0.38, 0.44 and 0.49 are obtained to be 521K, 569K, 590K and 674K, respectively.

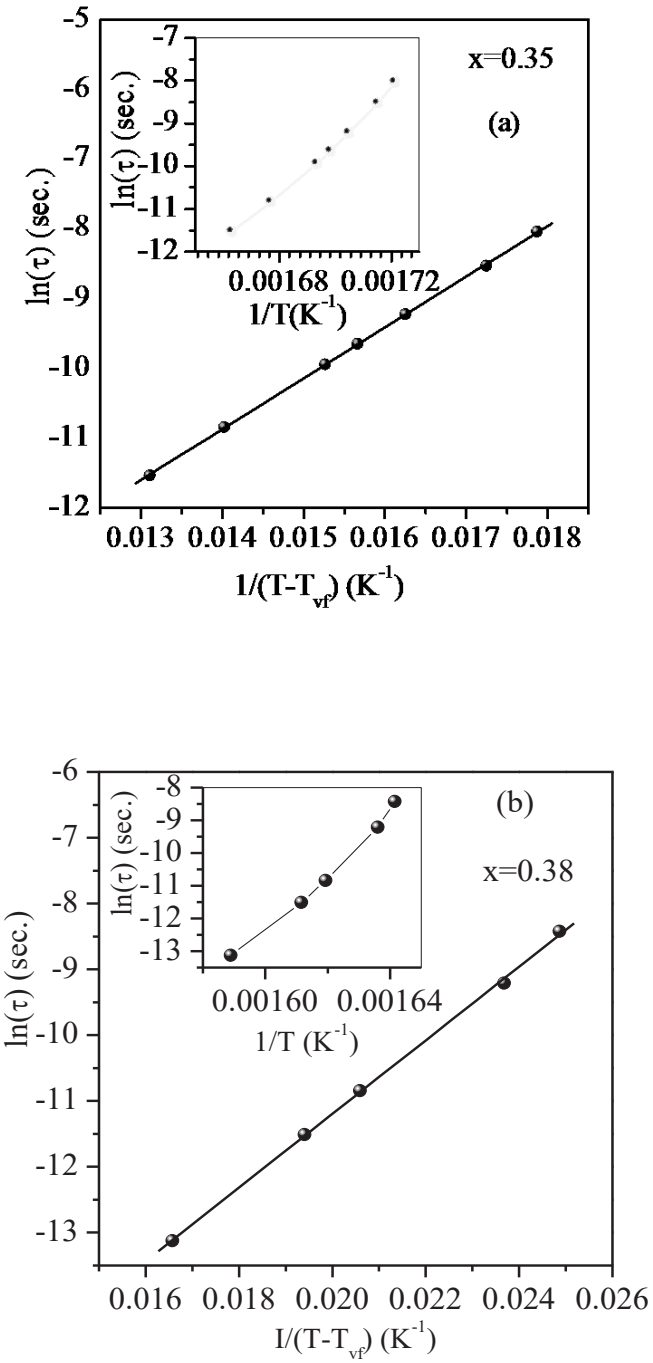

Fig.5.9.(a-b) Arrhenius (inset) and Vogel-Fulcher fits of the relaxation time, as obtained from the $\varepsilon^{/}$(T) data for the compositions with x=0.35 and 0.38. Linear fit is obtained for Vogel-Fulcher relation.

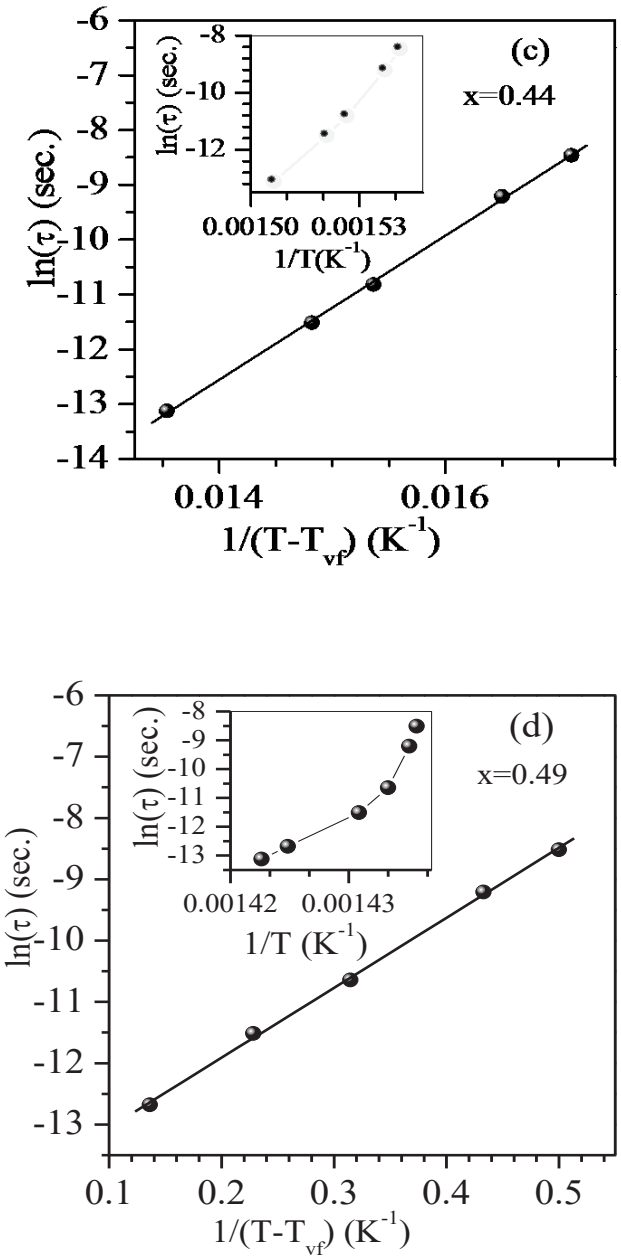

Fig.5.9.(c-d) Arrhenius (inset) and Vogel-Fulcher fits of the relaxation time, as obtained from the $\varepsilon'(T)$ data for the compositions with x=0.44 and 0.49. Linear fit is obtained for Vogel-Fulcher relation.

5.4. Discussion

Dielectric relaxation at high temperature around T_c is usually observed in the disordered systems such as $Pb(Mg_{1/3}Nb_{2/3})O_3$ [Smolenskii et al. (1961)] $Pb(Sc_{1/2}Ta_{1/2})O_3$ [Chu et al. (1993)], $Ba(Ti_{1-x}Sn_x)O_3$ [Yasuda et al. (1996)], $Ba(Ti_{1-x}Zr_x)O_3$ [Sciau et al. (2000); Simon et al (2004)] etc due to the presence of different size of cations at the same crystallography sites. This leads to the appearance of nanopolar regions of various length scales in such materials. Such materials transform to nonferroelectric (paraelectric) state well above the transition temperature similar to the normal ferroelectrics. This paraelectric state transforms in ergodic relaxor state on lowering the temperature below Burns temperature (T_B), the temperature, which is much more above the transition temperature (T_c) and not associated with any structural phase transition [Burns and Dacol, (1983)]. In ergodic relaxor state, polar regions of nanometer length scale have randomly oriented dipoles which are mobile near T_B [Burns and Dacol, (1983), Bokov and Ye, (2006)]. On further cooling below T_B, the polar nano regions (PNRs) get frozen into nonergodic relaxor state at the temperature T_f ($T_f < T_m$) with large and wide peak in the dielectric constant without affecting the average symmetry of the crystal which remains cubic in canonical relaxors [Bokov and Ye, (2006)]. The interesting point with this nonergodic relaxor state is that it can be transformed into ferroelectric phase by applying external electric field which is completely irreversible. This ferroelectric phase transform into ergodic state with randomly distributed PNRs on heating at T_c [Bokov and Ye, (2006)]. However, dielectric relaxation is also found in the systems where the

average symmetry is not cubic at room temperature. Dielectric relaxation in such systems also originates from disordered structure but they exhibit structural phase transition from paraelectric cubic phase to ferroelectric phase at T_c.

The origin of dielectric relaxation at low temperature is still a question of debate and no satisfactory explanation has been given by the researchers. As discussed earlier, various models have been proposed to understand the dielectric relaxation at low temperatures [Lente et al. (2004); Guo et al. (1990); Lente et al. (2004); Singh et al. (2007); Viehland (2000); Priya et al. (2002)]. Singh et al. (2007) have reported that the possible reason for the dielectric anomaly at cryogenic temperatures is due to formation of miniaturized monoclinic domains within each tetragonal domain [Singh et al. (2007)]. These miniaturized monoclinic domains are of mesoscopic scale and exhibit dielectric relaxation below room temperature due to thermal fluctuations. In present work, we have shown that there is no clear signature of structural phase transition below room temperatures. Therefore, the presence of fractal clusters in the normal ferroelectric region might be responsible for these anomalies. However, the dielectric relaxational peaks are present in all the tetragonal, monoclinic and cubic compositions and there will not be any ferroelectric region in cubic compositions. Thus, more investigations in future will be needed to understand the correct origin of these anomalies.

5.5 Summary

Different compositions of BNT-PT across MPB were characterized for the first time for their low temperature dielectric behaviour. Dielectric anomaly at

cryogenic temperatures is seen in all the compositions irrespective of their crystal structure at room temperature. Dielectric relaxation above as well as below room temperatures obeys Vogel-Fulcher law of freezing. Structural characterization of BNT-PT below room temperature shows that there is no structural transition in any of the composition at cryogenic temperatures. Thus, dielectric anomaly at cryogenic temperatures in BNT-PT is not originating due to structural transitions and may have some other origin. The relaxor behaviour above room temperature diminishes towards the tetragonal compositions but the low temperature relaxation is observed for all the compositions in the composition range $0.35 \leq x \leq 0.55$.